Thermal Analysis of He II-cooled Nb3Sn Superconducting Coil Samples for the HL-LHC Particle Accelerator Project

Kirtana Puthran

kirtana.puthran@cern.ch

Central Cryogenics Laboratory,
Cryogenics Research Group
TE-CRG-CI, CERN

Contributors:
Lise Murberg
Patricia Borges de Sousa
Rob van Weelderen
Torsten Koettig

Goals

In context of thermal behaviour of the 11T dipole (D11T) and inner triplet quadrupoles (MQXF) for HiLumi LHC,
an ongoing test program at the Cryolab at CERN;

1. **Experimental campaign** to measure thermal behavior of magnet samples.
2. Evolution of a robust multi-region end to end **numerical toolkit**.

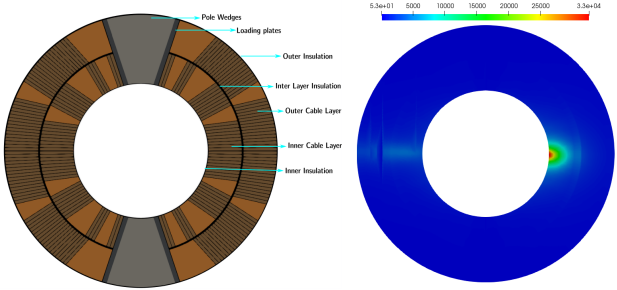

Coil Layer	Peak Power Dep. $\mathrm{mW/cm^3}$
Inner	32.9237
Outer	3.8166

2760 bunches with 2.3E11 protons/bunch, 8.81E11 protons/s loss rate

Courtesy: Andreas Waets, Anton Lenchner; SY/STI/CERN

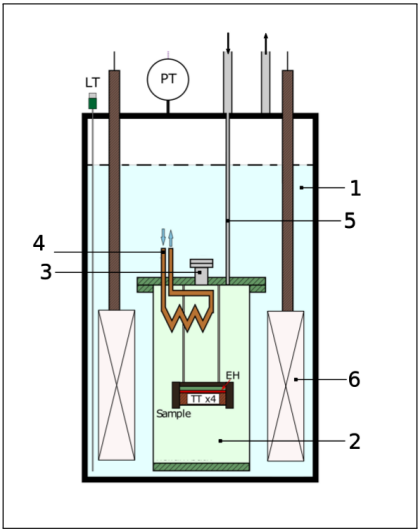

Aims to replicate the conditions as seen by the magnet coils in operating conditions, with two sample heating methods

- Vertical cryostat, with two separated volumes of liquid helium.
  - ⇒ Outer saturated bath [1]
  - ⇒ Inner pressurised bath (with sample), in G11 pot [2]
- Burst Disc [3]
- Temperature control via. Cu heat exchanger [4]
- Pressurisation control [5]
- External NbTi Magnet, for AC loss gen. method [6]

- Section of the coil predicted to experience the peak heat loads is chosen for cutting out the sample.
- Four holes of typically 1.4 mm diameter for each of the temperature sensors (Cernox^{TM} bare-chip) are carefully drilled into the cable layers at equal lengths from the ends such that the sensors can be placed in the center of the cable layer cross section.
- Samples insulated to allow only inner surface in direct contact with He II.

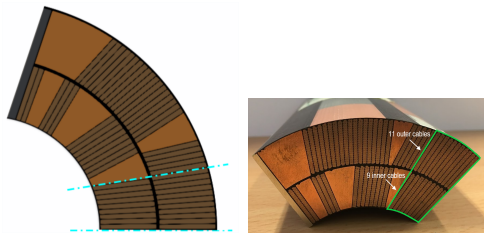

Quarter section from Coil GE02 as obtained.
Section cut out as sample marked.

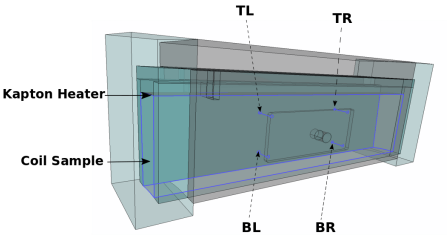

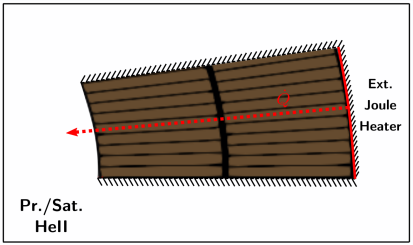

External heating

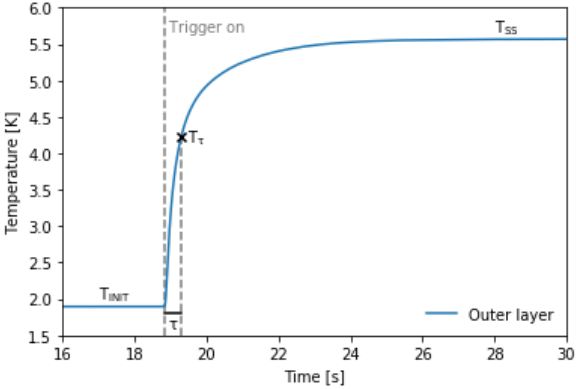

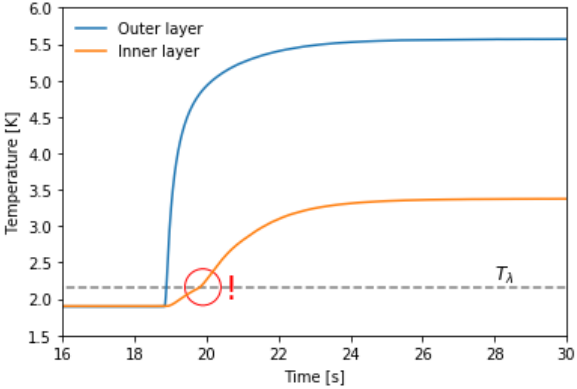

Typical measurement for each heat input, at a given bath temperature

1. Steady state temperatures :
   Provides indication of temperature rise of cable layers.
2. Time constants :
   Provides indication of heat capacities involved, i.e. 'helium content'.

→ Inner Surface heat-exchange coefficients:
Steady state T-differences with respect to helium bath as function of average temperature.

→ Inter layer heat-exchange coefficients:
Steady state T-differences between the coil layers allows for insulation material data comparison.

→ Kapitza Conductance

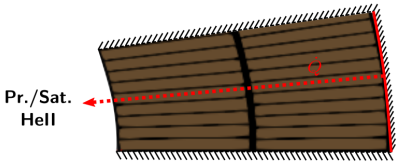

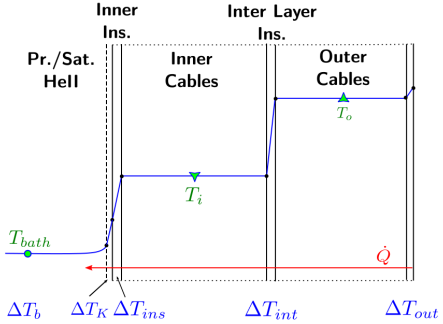

Experiment Results

Steady State Behaviour

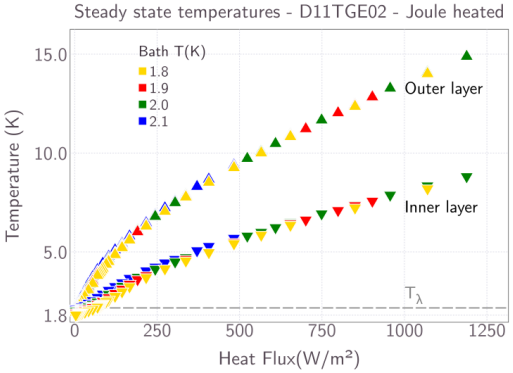

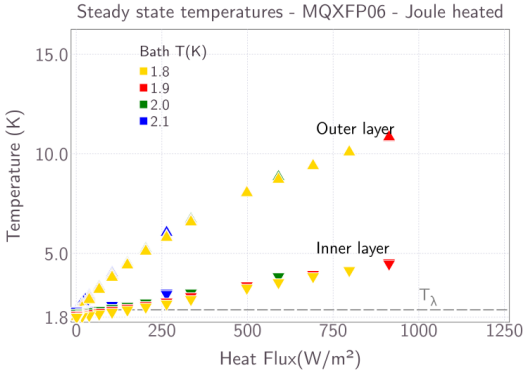

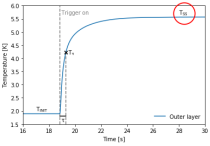

- At low heat loads $\approx 250 \mathrm{W/m^2}$, effect of bath temperature pronounced.
- At high heat loads, $\Delta\, T$ temperature irrespective of bath temperature (see extracted transfer coeffs., slide)
- Difference in curvature for inner cable layer at low[1]and high heat load, an indication of effect of helium, elaborated in data analysis slides.

[1] See Appendix

Experiment Results

Transient Behaviour

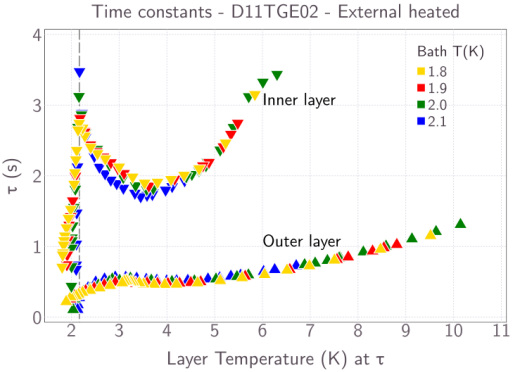

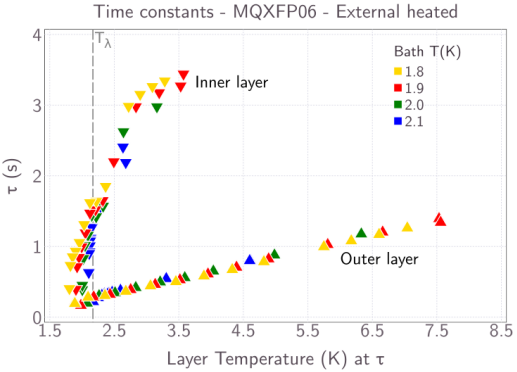

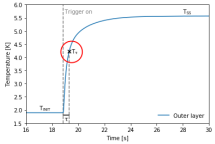

- For GE02, inner layer peak at T_λ with time constants up to 3.44 s, indicating He II presence, No indication of He II presence in outer layer.
- For P06, no indication of He II presence in both layers.

Data Analysis - 1

Approx. transfer coefficients/conductivity of inter layer insulation

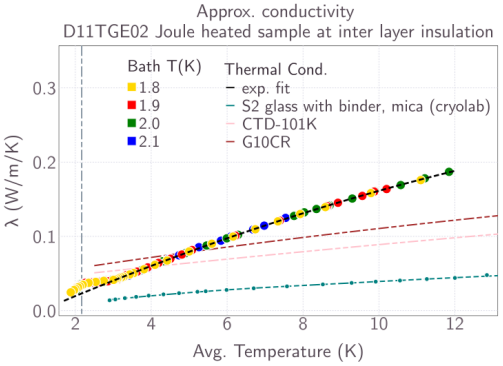

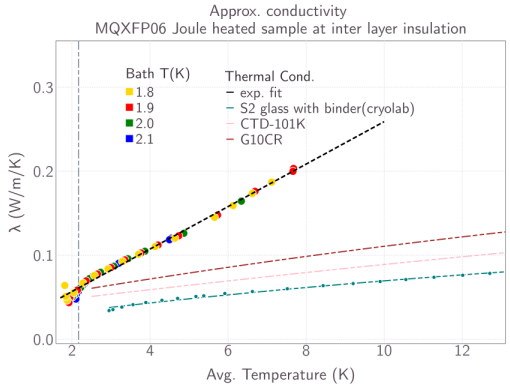

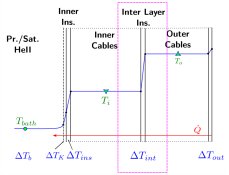

- Conductivity of interlayer insulation estimated from steady state temp. measurements and measured dimensions show deviation from material data.
- Difference in inter-layer insulation conductivity between the magnet coil samples, is larger than expected.

→ Possible factors? Type/components of glass fibre, VPI, curing, compression load, interface resistances...

Data Analysis - 2

Transfer coefficients at inner insulation

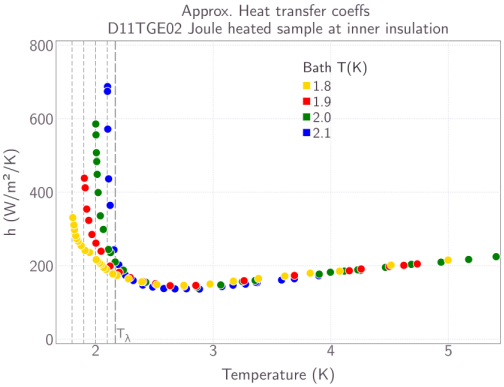

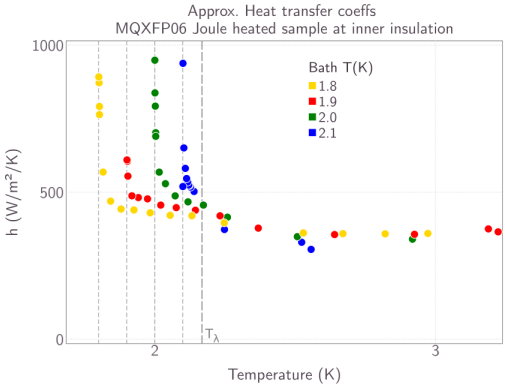

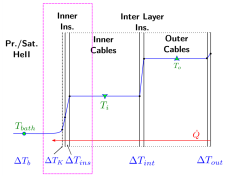

- Below 3 K, effect of Kapitza conductance or helium presence either within the inner insulation is predominant, or both.
- At average temperatures higher than 3 K, convergence in transfer coefficient.
- D11T sample shows lower transfer coefficient than MQXF sample (about factor 2), contrary to as expected from only a dimensional difference.

Data Analysis - 3

Kapitza Resistance Fits

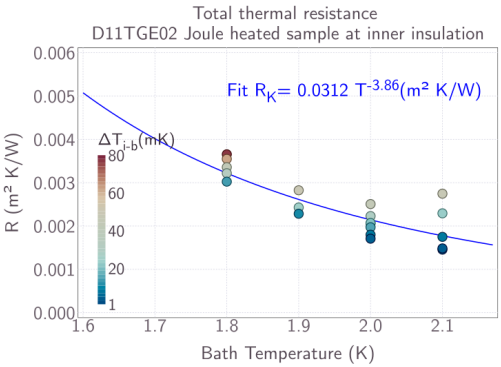

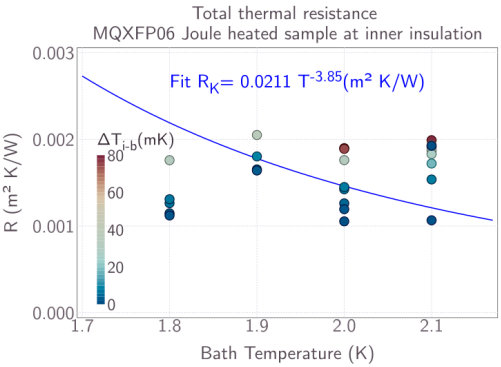

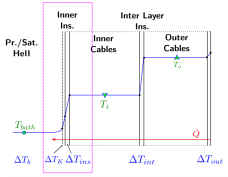

- At very low fluxes, ΔT_K dominates the contribution to ΔT_{inn}.
- Assuming fairly constant resistance, $R_K = A\frac{\Delta T_K}{\dot{Q}}$ for $\Delta T_K < 80\,mK$, kapitza transfer coefficient at inner surface can be estimated, using power fits ($\mathrm{AT^{-n}}$).

→ Resistance fits are over estimated for these samples, since surface temp. is not truly known without accurate material data and assumed Kapitza resistance domination.

- Geometry, Mesh
- Solver $\rightarrow$ Conjugate heat transfer; Static HeII, Solid (OpenFOAM)
- Special boundary conditions
- Low temperature material properties
- Convergence criteria
- Simulation time $\rightarrow$ Parallel computing
- Helium content in solid regions
- Validation of model
- Extrapolation to full magnet cross-sections to simulate peak power deposition scenarios.

1. For steady state heat transport, from two-fluid model, if no net mass flow;

$$\nabla T = -\frac{\beta \mu_n q}{d^2 (\rho s)^2 T} - f(T,p) q^m \qquad (1)$$

where,

$$K_L = -\frac{d^2 (\rho s)^2 T}{\beta \mu_n} \qquad (2)$$

$$K_{eff-GM} = \left(\frac{f^{-1}(T,p)}{|\nabla T|^2} \right)^{\frac{1}{m}} \qquad (3)$$

Sato's correlation[2], with m = 3.4:

$$f^{-1}(T,p) = h(t) g_{peak}(p) \qquad (4)$$

Energy equation :

$$\rho C_p(p,T) \frac{\partial T}{\partial t} = \nabla \cdot K_{eff} \nabla T \qquad (5)$$

? For wide channels, normal fluid viscous term is neglected, but initial singularity due to $|\nabla T|$!

× Introducing small initial gradient leads to numerical errors.

◇ Search for a critical gradient by equating laminar and turbulent regimes' gradient, but β and d for laminar regime is defined for specific geometries, plus in reality, a transition regime exists.

- For solid regions, standard heat conduction equation ;

$$\rho C_p(T)\frac{\partial T}{\partial t} = \nabla \cdot (k(T)\nabla T) + \dot{q} \tag{6}$$

Possibilities:

- HeII in porous media (Macroscopic model)
  → Pore size or porosity, permeability, specific surface area, tortuosity
- Conjugate heat transfer (Microsopic model)
  → Statistical distribution of shape and size, Kapitza, computationally v intensive.
- Phenomenological model for composite system
  → Surface/Volume Fraction of HeII
  1. Thermal conductivity[3](Semi-empirical model needed)

$$k = (1 - \phi_s)k_{solid} + \phi_s k_{HeII} \tag{7}$$

uses eqns. 4 & 5 for k_{HeII}

  2. Heat capacity

$$\rho C_p = (1 - \phi_v)(\rho C_p)_{solid} + \phi_v(\rho C_p)_{HeII} \tag{8}$$

[3] Progelhof, R. C., J. L. Throne, and R. R. Ruetsch. "Methods for predicting the thermal conductivity of composite systems: a review." Polymer Engineering & Science 16.9 (1976): 615-625.

Numerical Analysis

Parameter Evolution

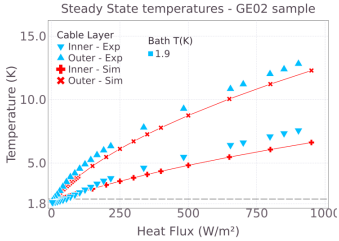

default

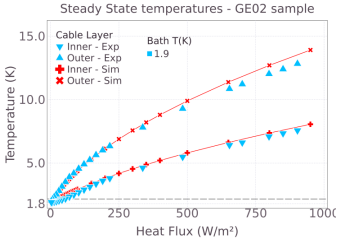

+ h_k + dim. + λ_{exp}

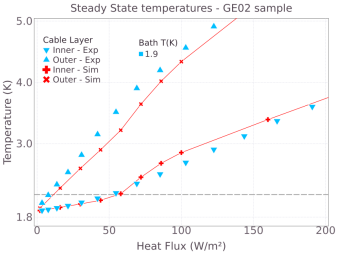

+ ϕ_s

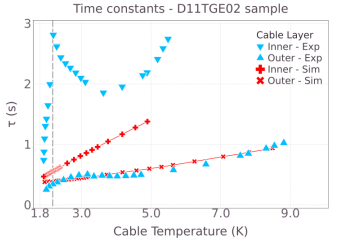

default

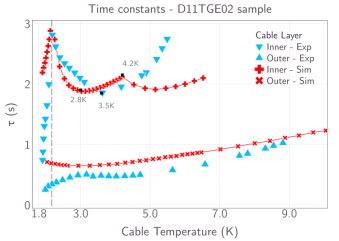

+ ϕ_v

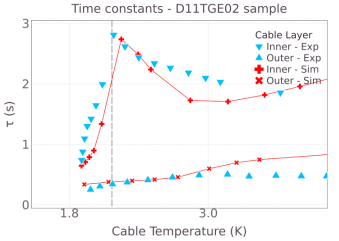

+ ϕ_s

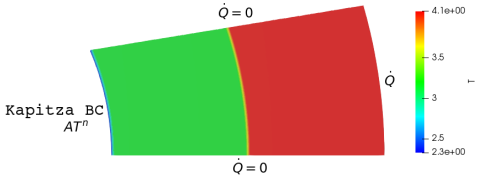

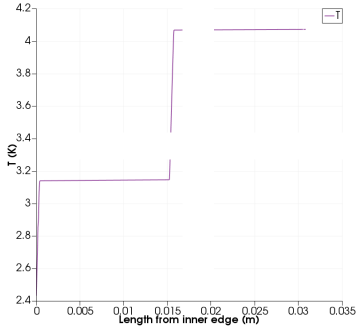

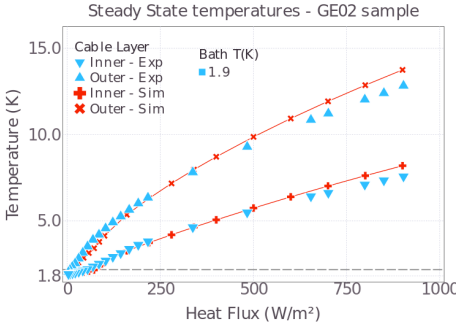

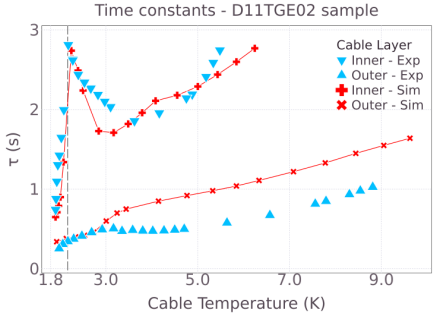

- Using measured coil sample characteristics, conservative estimates of max. temperature are made.

Simulation 2D

11T Full Coil at Peak Power Load : Temperature Map

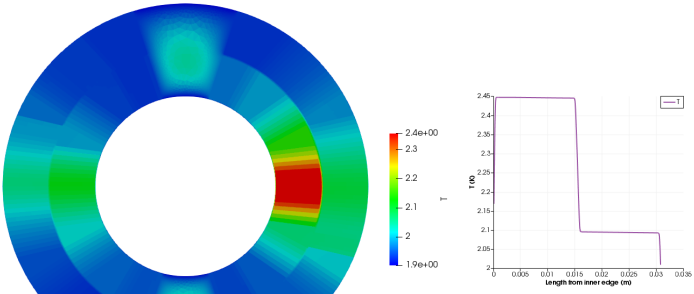

Nominal peak power $\approx 32 mW/cm^3$, heat map in slide 3

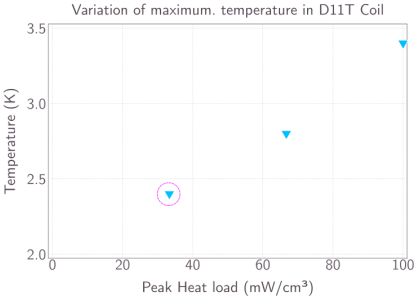

with factored heat maps

- Using measured coil sample characteristics, conservative estimates of max. temperature are made.
- Maximum coil temperature estimation for up to 3 times predicted peak load ($\approx 100\mathrm{mW/cm^3}$) remains within the temperature range of 1.9 K - 3.5 K. In the highest case, temperature margin of 1.6 K thus remains below design spec. of 4.5 K.

Summary

- ✓ Experiments can be used to estimate coil-specific parameters affecting the thermal behaviour and provide for a thorough validation of numerical models.
- ✓ Trace of helium content within the samples is evident through measured transient behavior.
- ? Literature data is incomplete for thermal conductivity, heat capacity of coil dielectric insulation materials and interface resistances. A semi-empirical description of the composite insulation would be most appropriate.
- ? HeII penetration might be a contributing factor to cable degradation, a known problem typical to Nb3Sn accelerator magnets $\rightarrow$ ongoing cyclic heat load experiments at cryolab.

Summary

- ✓ Numerical model developed with conjugate heat transfer between static superfluid helium and composite body, with Kapitza interface resistance has allowed for a qualitative analysis of factors affecting heat transfer behavior of the magnet coil samples, and extended to full coil pack geometry.
- ✓ Implementation of phenomenological model for helium content gives an estimate of helium penetration within the samples.
- ✓ Numerical analysis of the thermal transients estimates helium content of $\sim$ 0.35% in inner layer and $\sim$0% in outer layer of D11T coil samples, by volume fraction.
- ◇ Numerical toolkit could be upgraded with a more diverse experiment data set for validation and has potential to evolve into multi-physics capable.

Thank you!

Magnet Geometries

Drawing Cross-Sections

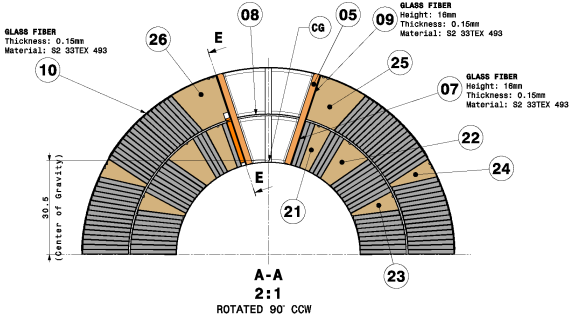

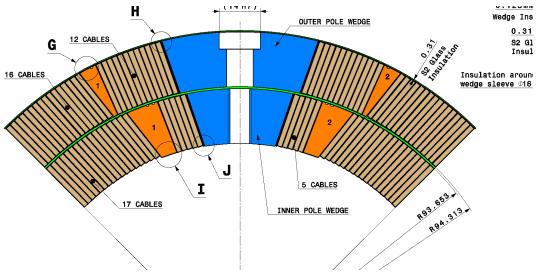

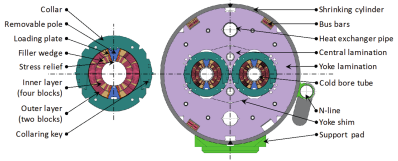

D11T

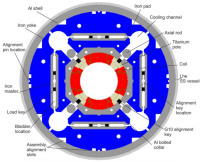

MQXF

Experiment Results

Steady State Behaviour

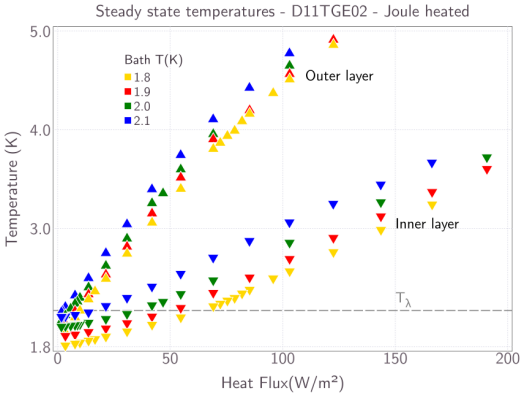

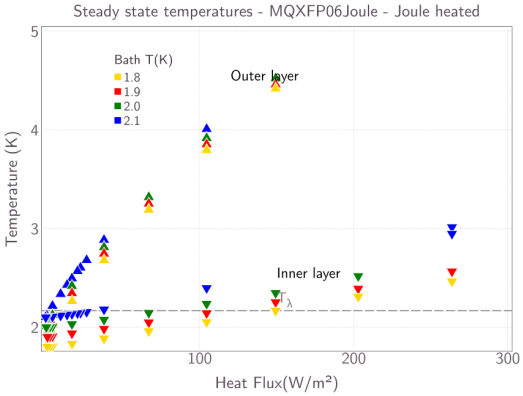

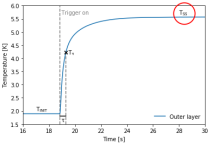

- Difference in curvature for inner cable layer at low and high heat load, an indication of effect of helium.

→ Resistance fits are over estimated for samples, since surface temp. is not truly known.

→ But, cannot be ignored for a good simulation.

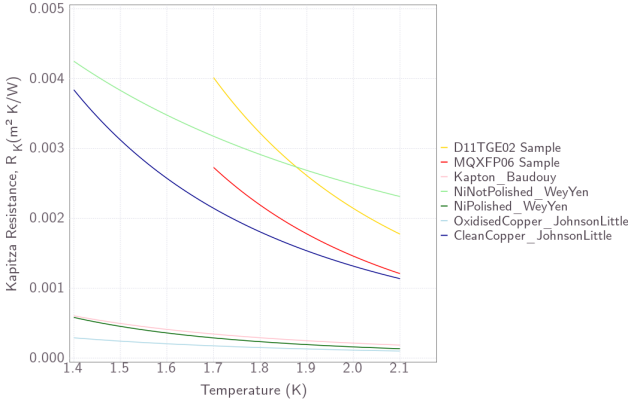

[4]Considering a symmetry of normal $\leftrightarrow$ superfluid mass transfer (to avoid defining an ill-posed problem), the momentum equations for the normal and superfluid components are respectively;

$$\frac{\partial \rho_n \mathbf{v}_n}{\partial t} + \nabla \cdot (\rho_n \mathrm{v}_n \mathrm{v}_n) = -\frac{\rho_n}{\rho}\nabla p - \rho_s s \nabla T + \nabla \cdot (\mu_n \nabla \mathbf{v}_n) - A \rho_n \rho_s |\mathbf{v}_n - \mathbf{v}_s|^2 (\mathbf{v}_n - \mathbf{v}_s) + [r_{ns}\mathbf{v}_s - r_{sn}\mathbf{v}_n] \quad (9)$$

$$\frac{\partial \rho_s \mathbf{v}_s}{\partial t} + \nabla \cdot (\rho_s \mathrm{v}_s \mathrm{v}_s) = -\frac{\rho_s}{\rho}\nabla p + \rho_s s \nabla T + A \rho_n \rho_s |\mathbf{v}_n - \mathbf{v}_s|^2 (\mathbf{v}_n - \mathbf{v}_s) - [r_{ns}\mathbf{v}_s - r_{sn}\mathbf{v}_n] \quad (10)$$

$\rho_s s \nabla T$ term represents the thermomechanical force which occurs due to a temperature gradient, responsible for creating counterflow of the components. Energy Conservation Equation, which is determined only by normal fluid is;

$$\frac{\partial \rho s}{\partial t} + \nabla \cdot (\rho s \mathbf{v}_n) = \nabla \cdot (\frac{k_n}{T}\nabla T) + \frac{A \rho_n \rho_s |\mathbf{v}_n - \mathbf{v}_s|^4}{T} \quad (11)$$

[4]Helium Cryogenics, Steven. W. Van Sciver